High specific capacitance supercapacitors from hierarchically organized all-cellulose composites

Mathias A. Hobisch,[a, b] Eléonore Mourad,[,b] Wolfgang J. Fischer,[a] Christian Prehal,[b] Samuel Eyley,[c] Anthony Childress,[d] Armin Zankel,[e] Andreas Mautner,[f] Stefan Breitenbach,[g] Apparao M. Rao,[d] Wim Thielemans,[c] Stefan A. Freunberger,[b,h] Rene Eckhart,[a] Wolfgang Bauer,[a] and Stefan Spirk[*,a]*

[a]Dr. M.A. Hobisch, Dr: W.J. Fischer, Dr. R. Eckhart, Prof. Dr. W. Bauer, Prof. Dr. S. Spirk
Institute of Bioproducts and Paper Technology,
Graz University of Technology,
Inffeldgasse 23, 8010 Graz, Austria
e-mail: stefan.spirk@tugraz.at

[b]Dr. E.Mourad; Dr. C. Prehal; Dr. S.A. Freunberger
Institute for Chemistry and Technology of Materials,
Graz University of Technology,
Stremayrgasse 9, 8010 Graz, Austria

[c]Dr. S. Eyley, Prof. Dr. W. Thielemans
Renewable Materials and Nanotechnology Research Group,
Katholieke Universiteit Leuven,
Etienne Sabbelaan 53, 8500 Kortrijk, Belgium

[d] Dr. A. Childress, Prof. Dr. A.M. Rao
Department of Physics and Astronomy, Clemson Nanomaterials Institute,
Clemson University,
Clemson, South Carolina 29634, USA

[e]Dr. A. Zankel
Institute of Electron Microscopy and Nanoanalysis, and
Graz University of Technology and Centre for Electron Microscopy,
Steyrergasse 17, 8010 Graz, Austria

[f]Dr. A. Mautner
Polymer and Composite Engineering (PaCE) group,
Department of Materials Chemistry,
University of Vienna, Währinger Straße 42, 1090 Vienna, Austria

[g]MSc. S. Breitenbach,
Wood K plus—Kompetenzzentrum Holz GmbH,
Altenberger Straße 69, 4040 Linz, Austria

[h] Prof. S.A. Freunberger
IST Austria (Institute of Science and Technology Austria), Am Campus 1,
3400 Klosterneuburg, Austria

Keywords: Carbon, Cellulose, Paper fines, Supercapacitor, EDLC, Electrochemistry

Abstract

Here, we employ micro- and nanosized cellulose particles, namely paper fines and cellulose nanocrystals, to induce hierarchical organization over a wide length scale. After processing them into carbonaceous materials, we demonstrate that these hierarchically organized materials outperform the best materials for supercapacitors operating with organic electrolytes reported in literature in terms of specific energy/power (Ragone plot) while showing hardly any capacity fade over 4,000 cycles. The highly porous materials feature a specific surface area as high as 2500 $m^{2} \cdot g^{-1}$ and exhibit pore sizes in the range of 0.5 to 200 nm as proven by scanning electron microscopy and N_2 physisorption. The carbonaceous materials have been further investigated by X-ray photoelectron spectroscopy and RAMAN spectroscopy. Since paper fines are an underutilized side stream in any paper production process, they are a cheap and highly available feedstock to prepare carbonaceous materials with outstanding performance in electrochemical applications.

1. Introduction

Increasingly large efforts and initiatives address the challenge of climate change by replacing fossil energy and petrochemical-based materials with sustainable resources.[1] Central to sustainability is the use of renewable, biobased materials along the whole production chain. In this context, lignocellulosics play a major role since they are highly abundant and already handled in large scale industries (e.g., paper and fiber manufacturers) exploiting different types of biobased materials such as wood and annual plants.[2] The main materials obtained from these industries are cellulosic pulps, lignins and hemicelluloses. Pulp production is accompanied by a variety of waste and side streams, which are currently not used for any material purpose. The most prominent ones are lignins, which still are the most unexploited material resource world-wide with nearly 98% being incinerated to generate thermal energy.[3] However, there are other only recently considered side streams containing cellulosic fiber fragments, named fines.[4] Fines are fibrous cellulosic microparticles (capable of passing through a 76 micron hole screen), which are formed in any cellulose processing industry such as papermaking and fiber manufacturing.[5] They are formed by mechanical or chemical treatments and therefore contain larger amounts of lignin than conventional paper pulps. Depending on their origin, primary and secondary fines are obtained with the major difference being their shape, size and extent of fibrillation.[6] Particularly secondary fines are highly interesting for paper manufacturers since they significantly improve the mechanical properties of paper.[7] Their aspect ratio combined with a larger share of amorphous domains compared to pulp fibers increases the bonded area between paper fibers.[8] Primary fines, however, are produced during the pulping process and primarily consist of ray cells and fragments from the primary cell wall, therefore showing a more flake-like morphology. They hardly contribute to paper strength and are detrimental for dewatering on the paper machine. Both primary and secondary fines take up or adsorb paper additives much faster and to a larger extent than pulp fibers. Consequently, removing fines from the process water cycles could reduce the paper

additive dosage and accelerate dewatering in paper production.[9] Since the speed of dewatering directly affects the runability of the paper machine and can also affect the dry content after the press section, any improvement in the removal of fines significantly impacts the production costs. Lately, methods have been developed to separate both types of fines from process waters in large scale.[10]

Since fines contain micro- and nanocelluloses, they may be useful for a variety of applications and could therefore be upcycled to high-value materials. In particular, electrode materials for supercapacitors are interesting applications, since the carbon source has a huge impact on performance and contributes a major fraction to the overall cost. These carbon materials could either be used as conductive additive in batteries or as electrode materials in supercapacitors (SCs). SCs are used in applications, where energy has to be delivered at high power for a rather short time, such as emergency exits in planes, bus doors, or as backup systems for mobile phones and laptops.[11] In the past, most of the supercapacitors built from biobased sources employed aqueous electrolytes.[12] These offer a higher capacitance than their counterparts with organic electrolyte but at the expense of lower operating voltages and shorter product life due to the aggressive nature of H_2SO_4 and KOH, the most commonly used electrolytes.

Here, we demonstrate that primary and secondary fines can be used as raw materials to produce carbonaceous materials for SC applications. The major challenge is to obtain activated carbons with high specific surface area (SSA) and a hierarchical pore size distribution, which we tackled by different activation procedures and the addition of cellulose nanocrystals. These materials are then used in supercapacitors with organic electrolytes and comprehensively characterized by electrochemical techniques.

2. Results and Discussion

The steps to prepare the supercapacitor involve (i) separating the fines from paper pulp, (ii) generating a porous cellulosic material, which is then (iii) activated, (iv) carbonized, and (v)

further assembled into a supercapacitor. Prior to these steps, the paper pulps were checked for impurities such as sulfur and metal ions, which could have negative effects on the supercapacitor performance. ICP-MS (Table S4) did not show any noticeable amounts of impurities.

2.1. Separating the fines from the paper pulp

First, the pulp was diluted with water to 1 wt.% solid content and then transferred to a pressure screen. The device was equipped with a perforated strainer with holes having a diameter of 100 µm. The fines fraction passed the strainer and was collected in a container while larger particles were retained and transferred back to the feed tank. Since the solids content of the obtained fines suspension was very low (0.02 wt.%), a laboratory flotation cell was directly connected to the separation device to increase the solids content to 4 wt.%, which was then subjected to lyophilization. To avoid contamination of the material, flotation was done using dissolved air flotation without the use of any additives or surfactants. For further information on the separation device, the reader is referred to a recent publication.[10]

2.2. Pre-carbonization and activation

The major task of the present work was to increase the specific surface area (SSA) of the starting material (PCF, P1, 5 $m^2 \cdot g^{-1}$) to the targeted value beyond 1000 $m^2 \cdot g^{-1}$. The lyophilized fines were first pre-carbonized at 400 °C. After cooling to room temperature, the PCFs were mixed with base, $NaHCO_3$ or KOH, and carbonized at 800 °C to yield activated carbons (P2-P4, S1, S2, M1, M2).

The pre-carbonized fines (PCF) sample P1 showed a rather low surface area of 5 $m^2 \cdot g^{-1}$. The activation methods yielded much higher SSA ranging from 970 (P2, $NaHCO_3$) to 1385 $m^2 \cdot g^{-1}$ (P3, KOH, by BET). The secondary fines showed inferior results as compared to the primary fines in terms of the SSA (470 and 900 $m^2 \cdot g^{-1}$) and pore size distribution derived via non-local

density functional theory (NLDFT). Therefore, secondary fines have not been further investigated for the application in supercapacitors.

The SSA was further increased by adding rod shaped CNCs (**Figure S1,** 50 and 90 wt.%, denoted as M1 and M2,) to the primary fines suspensions. As indicated in **Figure 1a**, at 50 wt.% CNC content, the SSA increased to nearly 2580 $m^{2}\cdot g^{-1}$ after carbonization, while at 90 wt.% CNC the SSA had a lower value of 1540 $m^{2}\cdot g^{-1}$. A potential explanation for this involves accumulation of CNCs in voids between the fines at 50% CNC content, thereby creating a hierarchical structure at different length scales but also with different stiffness of the individual components. Upon activation, these two structures seem to result in smaller pores yielding markedly higher SSA than the carbonized fines. However, at high CNC contents (90%), the fines intercalate between the CNCs. As for the sample with 50% CNC content, a hierarchical structure is formed which is less flexible due to higher stiffness of the CNC nanoparticles. Average pore sizes of the obtained carbons used in SCs were 1.4 (P3) and 0.548 nm (M1). N_2 physisorption results and the corresponding pore size graphs are shown in **Figure 1b,c**. A plausible explanation for a lower SSA with the high CNC fraction is pore blocking of the composite (Figure 1c, M2) as described for related cases.[13]

2.3. Morphology

Raman spectroscopy and XPS measurements were performed for further material characterization. The Raman spectra appeared mostly identical for all samples except for P3 which exhibits a *G*' band at ca 2700 cm^{-1}. This band is associated with the presence of ordered carbonaceous domains, while the other samples consist merely of amorphous carbon (**Figure 1d).** Further, lineshape analysis of the spectra in **Figure 1d** revealed the presence of two Lorentzians for samples M1 and M2. One appears at ~1350 cm^{-1} for the so-called disorder or *D*-band, and the other at ~1580 cm^{-1} for graphitic or the *G*-band. The ratio (*R*) of the D-band to G-band integrated intensity is a measure for the degree of disorder in the sample. Herein, M1 has the highest *R* value, leading to the highest specific capacitance of all samples. Further, the

XPS data for these samples (**Figure S3**, †ESI) provides good evidence for carbonization through higher carbon content post-carbonization relative to the primary fines. The elemental composition as determined using XPS is given in Table S6 and shows next to C between 15 (P3) and 10% (M2) O as the other main component. Silicon was present in all samples and can be traced back to the primary fines starting material (presumably in the form of silicates) as evidenced by the reduction in silicon content with increased CNC content. (Table S6)

The largely increased surface area after activation and carbonization was accompanied by a morphological transformation. The pre-carbonized samples (PCF) showed a mesoporous structure (**Figure S2**, †ESI) as determined by LV-SEM. Additional micropores were formed by various activation protocols used during carbonization. SEM images after activation with KOH showed pores between 10 to 200 nm (**Figure 2**) pointing out the hierarchical organization of the pore structure.

2.4. Electrochemical performance

We assembled symmetric supercapacitors in a three-electrode configuration to assess the electrochemical parameters such as specific capacitance and resistance of the synthesized electrode materials. Since manually-formed electrode masses vary, an overview is given in Table S1-S3 on the amount of active material in the electrodes.

Cyclic voltammetry (CV) at a scan rate of 10 $mV \cdot s^{-1}$ showed a typical rectangular shape, pointing at an ideal EDLC behavior with all electrode materials, including the reference (**Figure 3a**). Accordingly, galvanostatic cycling revealed linearly rising and falling potentials on charge/discharge with a voltage drop upon change in current direction stemming from internal resistance (**Figure 3b**). Herein, variations in the electrode weight impacted charging and discharging time during galvanostatic cycling (Equation (1)[14]**):**

$$C_{S,Electrode} = 2 \cdot \frac{\int_{V_i}^{V_f} i \cdot dV}{\Delta V \cdot v \cdot m} \qquad (1)$$

with C_s being the specific capacitance, $\int_{V_i}^{V_f} i \cdot dV$ the integral over the positive part of the CV curve between the maximum and minimum, V_f and V_i, of the cell voltage ΔV, V the potential, v the scan rate and *m* the mass of active material in the two electrodes. The specific capacitance ranged from 130 (P3), 156 (M1), and 146 $F \cdot g^{-1}$ (M2) at 2 $mV \cdot s^{-1}$, which was higher than the reference (YP-80F) with 111 $F \cdot g^{-1}$. The materials containing CNCs featured significantly larger capacitance than than the purely fine-based materials regardless of the electrode loading which originates from the higher SSA of 2580 and 1540 *vs.* 1385 $m^2 \cdot g^{-1}$ for M1, M2 and P3, respectively. The voltage drop at the turning points was caused by the Ohmic drop, which allowed for calculating the resistance of the whole cell. The various activated fines had an average pore size of 1.41 (P3), and 0.55 nm for both, M1 and M2. Although in average M1 and M2 showed the same pore width, there were significant differences in pore volume and surface area, which had less influence on the specific capacity than previously expected. SC performance is not solely determined by porosity and pore size distribution but also by electrode conductivity and overall resistance. EIS measurements revealed that M1 and M2 have lower electrode resistances than P3. Slight discrepancies were observed in the diffuse layer resistance, where M2>M1>P3. A further decreasing the frequency did not affect the resistance of the samples. (**Figure S4**, †ESI)

Long-term cycling over 4,000 cycles at ~0.6 $A \cdot g^{-1}$ revealed a capacity retention of nearly 100% for all the samples including the reference (P3:101%, M1: 96%, M2: 98%, YP-80F:100%, **Figure 3c)**. The capacitance increase for P3 (from 113 to 115 $F \cdot g^{-1}$) pointed at reorientation of the activated carbons during cycling[15]. The capacitance retention upon variation of the scan rate from 2 – 100 $mV \cdot s^{-1}$ was more pronounced for the samples containing CNCs (M1, M2, **Figure 3d**).Upon faster charge-discharge cycles, a fraction of the smaller pores in these materials cannot participate in charge transfer, thereby reducing capacitance. In contrast, the

reference material performed best in this respect with 78% capacitance retention at 100 $mV \cdot s^{-1}$, however at the price of lower capacitances at low cycling rates (2 $mV \cdot s^{-1}$).

The Ragone plot showed remarkable values for specific power and energy for all our materials compared to literature values. A specific energy of ~50 $Wh \cdot kg^{-1}$ at a specific power of 10,000 $W \cdot kg^{-1}$ in organic electrolytes can be considered as excellent value in literature, which however is difficult to compare as the experimental setup and electrode mass/active material may vary, directly impacting reported performance.[16] Therefore, we used the industrial reference (YP-80F) to benchmark our system and prepared electrodes with similar amounts of active material **(Table S1**). At 10,000 $W \cdot kg^{-1}$ the fines-based materials perform slightly worse or similar than the reference (45, 55, 60 for P3, M1, M2 vs 65 $Wh \cdot kg^{-1}$ for YP-80F, **Figure S5**). At power densities lower than 5,000 W kg^{-1}, M1 and M2 revealed higher energy densities than the industrial benchmark. In general, CNC containing activated fines have higher specific energies than those without CNCs due to denser packing of the electrode, leading to higher capacitance, and better conductivity. The higher conductivity of M2 compared to M1 and P3 translates to higher specific energy despite the smaller SSA and capacitance of M2.

3. Conclusion

In conclusion, fines obtained from an abundant side stream of paper industry have been exploited as supercapacitor electrode materials. The fines were first separated from paper pulp using an ecologically friendly and scalable technology and then subjected to pre-carbonization either with or without addition of commercially available cellulose nanomaterials (CNC). Activating pre-carbonized fines gave access to very high specific surface areas up to 2500 $m^2 \cdot g^{-1}$, which were suitable for supercapacitor applications. The electrochemical performance of the materials in supercapacitors with organic electrolytes yielded values of up to 156 $F \cdot g^{-1}$ at a scan rate of 2 $mV \cdot s^{-1}$, which is in the upper range of values reported for activated carbons using organic electrolytes.

The fines-based electrodes appear to feature favorable pore sizes for both long-range transport and high capacitance and are at least at par with the commercial YP-80F carbons as shown in the Ragone plot. Upcycling fines, a readily available and highly abundant low-value side stream in paper industry, into high-value electrode materials provides thus an excellent possibility to enhance sustainability and economics in paper industry and energy storage at the same time. Currently, we undertake efforts to elucidate the costs of potential processes (with and without additional CNCs) at different scales and try to assess the life cycle of the production procedure.

Supporting Information

Supporting Information is available from the Wiley Online Library or from the author. Experimental procedures and details (AFM, SEM, elemental analysis using XPS and ICP-MS, Figure S1-S5, Table S1-S4).

Acknowledgements

The authors M.A.H., S.S., R.E., and W.B. acknowledge the industrial partners Sappi Gratkorn, Zellstoff Pöls and Mondi Frantschach, the Austrian Research Promotion Agency (FFG), COMET, BMVIT, BMWFJ, the Province of Styria and Carinthia for their financial support of the K-project Flippr²-Process Integration. E.M. and S.A.F. are indebted to the European Research Council (ERC) under the European Union's Horizon 2020 research and innovation program (grant agreement No 636069). W. T. and S. E. thank FWO (G.0C60.13N) and the European Union's European Fund for Regional Development and Flanders Innovation & Entrepreneurship (Accelerate3 project, Interreg Vlaanderen-Nederland program) for financial support. W. T. also thanks the Provincie West-Vlaanderen (Belgium) for his Provincial Chair in Advanced Materials. S. B. thanks the European Regional Development Fund (EFRE) and the province of Upper Austria for financial support through the program IWB 2014-2020 (project BioCarb-K). AMR gratefully acknowledges funding support through the SC EPSCoR/IDeAProgram under Award #18-SR03, and the NASA EPSCoR Program under Award #NNH17ZHA002C. Icons in Scheme 1 were provided by Good Ware, monkik, photo3idea_studio, and OCHA from www.flaticon.com.

Received: ((will be filled in by the editorial staff))
Revised: ((will be filled in by the editorial staff))
Published online: ((will be filled in by the editorial staff))

References

[1] M. D. Tabone, J. J. Cregg, E. J. Beckman, A. E. Landis, *Environ. Sci. Technol.* **2010**, *44*, 8264.
[2] M. A. Hubbe, R. A. Venditti, O. J. Rojas, *BioResources* **2007**, *2*, 739.
[3] M. Kosa, A. J. Ragauskas, *Green Chem.* **2013**, *15*, 2070.

[4] a) M. Mayr, R. Eckhart, W. Bauer, *Nord. Pulp Pap. Res. J.* **2017**, *32*, 244; b) M. Bäckström, M.-C. Kolar, M. Htun, *Holzforschung* **2008**, *62*, 546.
[5] N. Odabas, U. Henniges, A. Potthast, T. Rosenau, *Prog. Mater Sci.* **2016**, *83*, 574.
[6] K. Hyll, *Nord. Pulp Pap. Res. J.* **2015**, *30*, 466.
[7] T. Taipale, M. Österberg, A. Nykänen, J. Ruokolainen, J. Laine, *Cellulose* **2010**, *17*, 1005.
[8] W. J. Fischer, A. Zankel, C. Ganser, F. J. Schmied, H. Schroettner, U. Hirn, C. Teichert, W. Bauer, R. Schennach, *Cellulose* **2013**, *21*, 251.
[9] R. Giner Tovar, W. J. Fischer, R. Eckhart, W. Bauer, *BioResources* **2015**, *10*, 7242.
[10] W. Fischer, M. Mayr, S. Spirk, D. Reishofer, L. Jagiello, R. Schmiedt, J. Colson, A. Zankel, W. Bauer, *Polymers* **2017**, *9*, 366.
[11] P. Simon, Y. Gogotsi, *Nat. Mater.* **2008**, *7*, 845.
[12] a) S. Y. Liew, W. Thielemans, D. A. Walsh, *J. Solid State Electrochem.* **2014**, *18*, 3307; b) S. Y. Liew, W. Thielemans, D. A. Walsh, *J. Phys. Chem. C* **2010**, *114*, 17926; c) S. Y. Liew, D. A. Walsh, W. Thielemans, *RSC Adv.* **2013**, *3*, 9158; d) S. Y. Liew, W. Thielemans, S. Freunberger, S. Spirk, *Polysaccharide Based Supercapacitors*, Basel, Springer International, 2017.
[13] X. Xu, J. Zhou, L. Jiang, G. Lubineau, T. Ng, B. S. Ooi, H. Y. Liao, C. Shen, L. Chen, J. Y. Zhu, *Nanoscale* **2016**, *8*, 12294.
[14] R. de Levie, *Electrochim. Acta* **1963**, *8*, 751.
[15] a) D. V. Lam, K. Jo, C. H. Kim, J. H. Kim, H. J. Lee, S. M. Lee, *ACS Nano* **2016**, *10*, 11351; b) T. Qin, S. Peng, J. Hao, Y. Wen, Z. Wang, X. Wang, D. He, J. Zhang, J. Hou, G. Cao, *Adv. Energy Mater.* **2017**, *7*, 1700409.
[16] D. Wang, S. Liu, L. Jiao, G. Fang, *Electrochim. Acta* **2017**, *252*, 109.

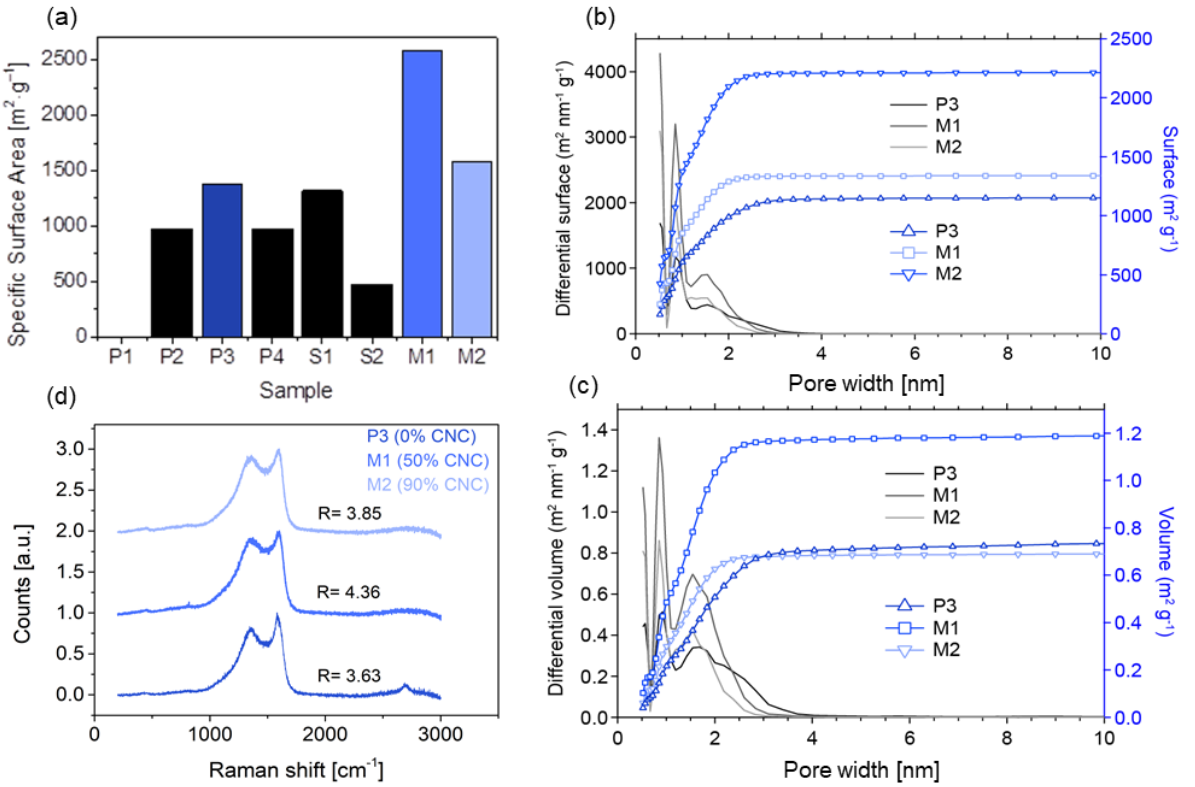

Figure 1. (a) Specific surface area of differently activated carbons as obtained from N_2 physisorption for primary (P), secondary (S) and composite (M) fines. P1: no activation, P2: $NaHCO_3$, P3, P4, S1, S2, M1, M2: KOH. Note that P3, S1, M1 and M2 have been prepared by homogenizing KOH with the preactivated carbons, while P4 and S2 were not homogenized with the KOH. The bluish colored materials are further investigated in this manuscript (P3, M1, M2). (b) Differential and cumulative pore size distributions weighted by pore volume (c) Differential and cumulative pore size distributions weighted by pore surface. (d) Raman spectra of the carbonized samples showing the experimental data of the samples (P3, M1, M2). The ratios (*R*) of the integrated intensities of the *D*-band to that of the *G*-band are also listed in the figure.

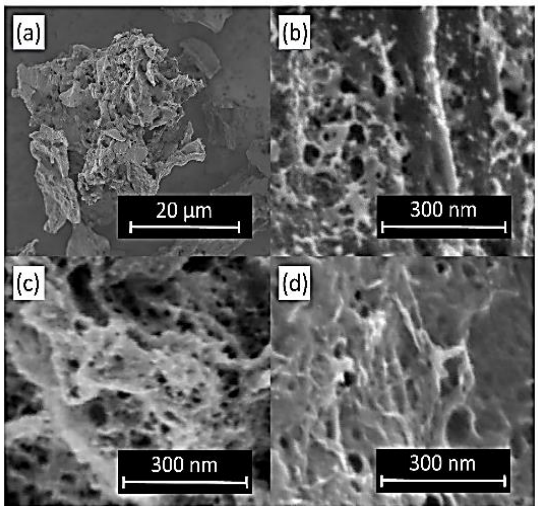

Figure 2. LV-SEM images of different carbonized primary fines and blends with CNCs. (a, b) P3, (c) M1 and (d) M2.

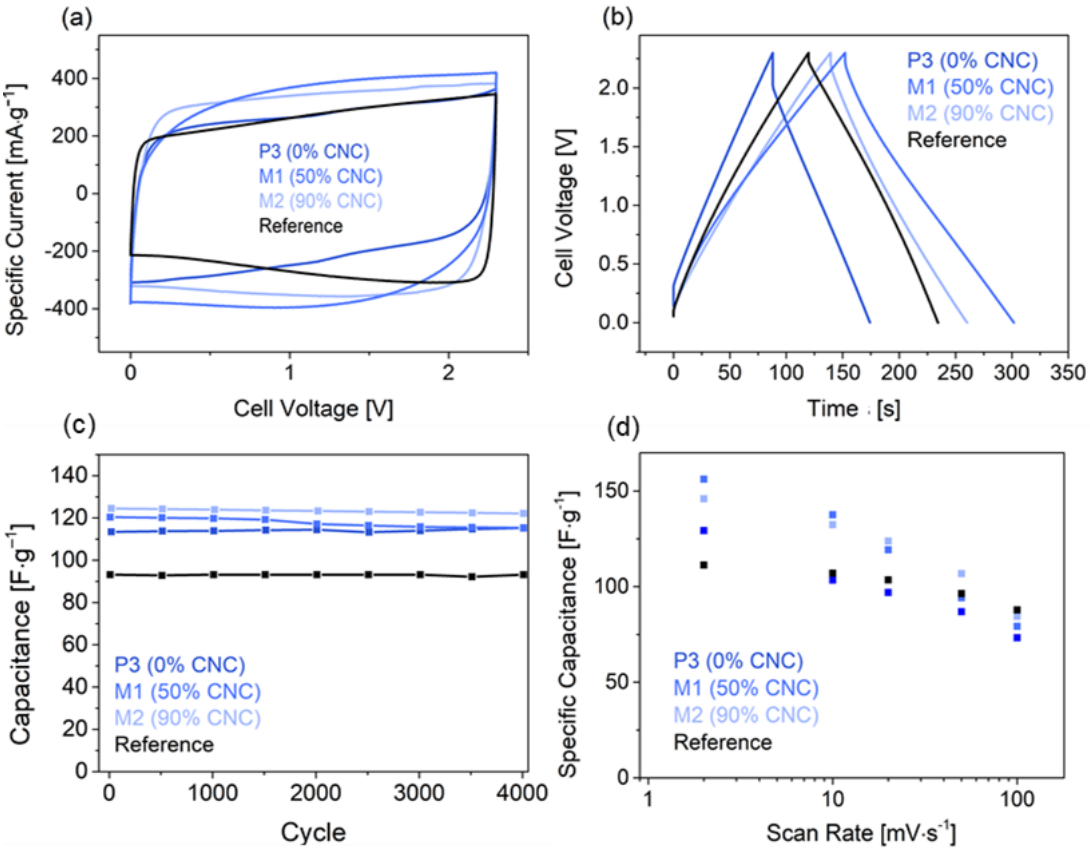

Figure 3. Electrochemical characteristics of the fines-based electrodes in symmetric supercapacitors (P3, M1, M2) and an industrial reference (YP-80F) in 1 M $TEABF_4$/AN as the electrolyte. (a) Cyclic voltammetry at a scan rate of 10 $mV \cdot s^{-1}$. (b) Galvanostatic cycling between 0 and 2.3 V at a constant current of 3 mA. (c) Cycling stability at 0.6 $A \cdot g^{-1}$. (d) Capacitance retention at different scan rates. Precise active material mass and total electrode mass are listed in Table S1 and S2.

High specific capacitance supercapacitors from hierarchically organized all-cellulose composites

*M.A. Hobisch, E.Mourad, W. J. Fischer, C.Prehal, S. Eyley, A. Childress, A. Zankel, A. Mautner, S. Breitenbach, A.M. Rao, W.Thielemans, S.A. Freunberger, R. Eckhart, W. Bauer, and S. Spirk**

Keywords: Carbon, Cellulose, Paper fines, Supercapacitor, EDLC, Electrochemistry

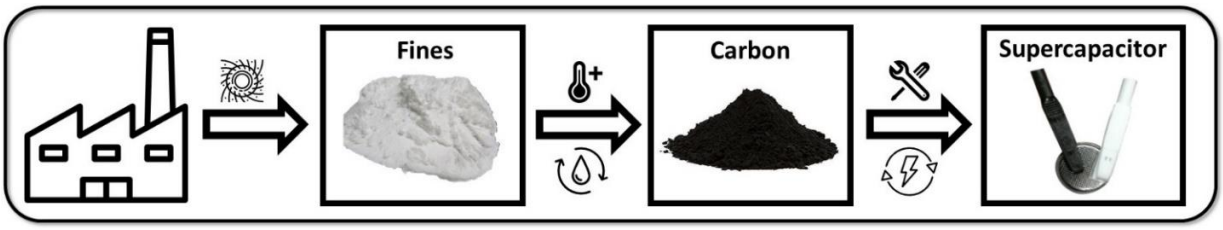

Black gold from white waste. The conversion of cellulose from an industrial side stream, cellulosic fines, into activated carbons yields high-performance supercapacitor electrodes. Assembling the electrodes in symmetrical supercapacitors using organic electrolytes reveals excellent electrochemical properties.